Reaction Pathway Control via Reactant Vibrational Excitation and Impact on Product Vibrational Distributions: The O + HO$_2$ → OH + O$_2$ Atmospheric Reaction

Qixin Chen, Shuwen Zhang, Xixi Hu,* Daiqian Xie, and Hua Guo

ACCESS | Metrics & More | Article Recommendations | SI Supporting Information

ABSTRACT: Chemical reactions often have multiple pathways, the control of which is of fundamental and practical importance. In this Letter, we examine the dynamics of the O + HO$_2$ → OH + O$_2$ reaction, which plays an important role in atmospheric chemistry, using quasi-classical trajectories on a recently developed full-dimensional potential energy surface (PES). This reaction has two pathways leading to the same products: the H abstraction pathway (O$_a$ + HO$_b$O$_c$ → O$_a$H + O$_b$O$_c$) and the O abstraction pathway (O$_a$ + HO$_b$O$_c$ → O$_b$H + O$_a$O$_c$). Under thermal conditions, the reaction is dominated by the latter channel, which is barrierless, leading to vibrational excitation of the O$_2$ product. However, we demonstrate that excitation of the HO$_2$ reactant in its O−H (v_1) vibrational mode results in dramatic switching of the reaction pathway to the activated H abstraction channel, which leads to a highly excited OH product vibrational state distribution. The implications of such dynamical effects in the atmospheric chemistry are discussed.
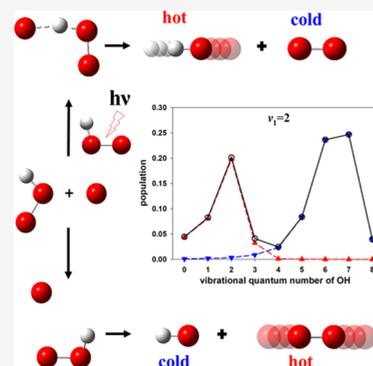
A holy grail in chemistry is the control of the product branching of a chemical reaction. The relative yields of various product channels are often influenced by the differing barrier heights in the corresponding pathways and dynamics could also play an important role.[1] The rapid progress of experimental and theoretical understanding of the dynamics of multichannel reactions in recent years has greatly advanced our understanding of the dynamical control of reactivity and product branching.[2−5] In a recent study, for example, the branching ratio between the CH$_3$O + HF and CH$_2$OH + HF channels in the F + CH$_3$OH reaction was investigated theoretically, and it was shown that stereodynamics has a more significant impact than energetics.[6]

In this Letter, we examine a slightly different scenario in which two reaction pathways lead to the same products, as manifested by the following reaction:

$$HO_2(X^2A'') + O(^3P) \rightarrow OH(X^2\Pi) + O_2(X^3\Sigma_g^-) \quad (R1)$$
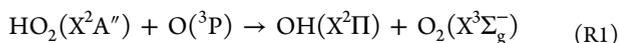
This radical−radical reaction is of great importance in atmospheric chemistry as it provides a key atomic oxygen destruction pathway in the stratosphere (215−270 K) and mesosphere (180−270 K) and plays a major role in controlling the partitioning among the HO$_x$ species.[7] The vibrational state distribution of the OH radical produced by reaction R1 could potentially influence an array of atmospheric phenomena. For instance, several authors have proposed that the nascent OH product may have significant vibrational excitation, thus responsible for hydroxyl night airglow.[8−11] However, this proposal has been disputed by others who believe that the OH

vibrational excitation is small.[12−15] Definitive evidence to resolve issues like this requires the determination of the OH vibrational distribution for the title reaction.

As shown in Figure 1, this exothermic reaction has two pathways.[16,17] The O abstraction (OA) pathway (O$_a$ + HO$_b$O$_c$ → O$_b$H + O$_a$O$_c$), featuring a submerged barrier (SP1), forms O$_2$ via abstracting the terminal oxygen of HO$_2$ (O$_c$) by the atomic oxygen (O$_a$), leaving the O$_b$H group as a spectator. The alternative H abstraction (HA) pathway (O$_a$ + HO$_b$O$_c$ → O$_a$H + O$_b$O$_c$), which has a small barrier (SP2), proceeds by abstracting the H atom from HO$_2$ by the atomic oxygen (O$_a$), with the O$_2$ moiety as a spectator. Although both pathways lead to nominally the same products, it is readily seen from Figure 1 that they are not expected to have equal contributions under thermal conditions, due to their different barrier heights. At conditions relevant to atmospheric chemistry, the OA channel dominates. Furthermore, it is clear from the transition state configurations that the products are likely to have different extents of vibrational excitation. Indeed, the O$_a$−O$_c$ bond length at SP1 is much larger than the one for oxygen molecule, which may produce highly vibrationally excited O$_2$, same for the OH radical in the HA pathway. As described
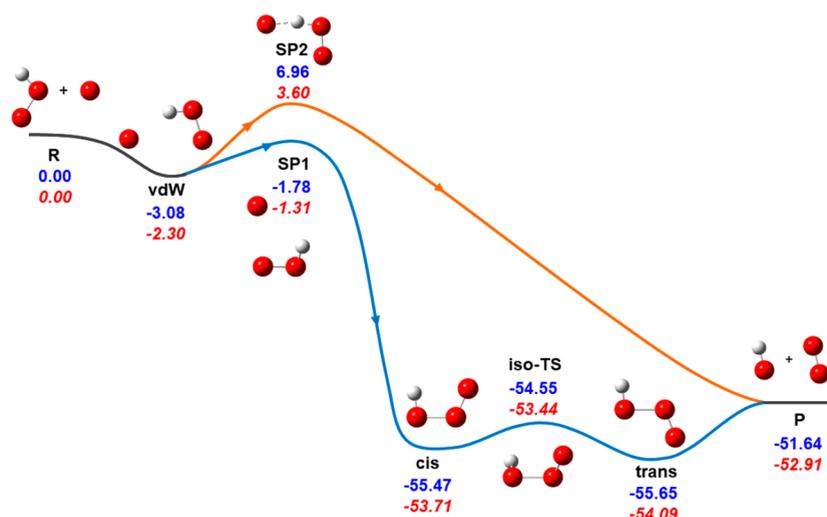
Figure 1. Energetics of the $HO_2 + O \rightarrow OH + O_2$ reaction on the HO_3 PES. The energies are relative to the $HO_2 + O$ asymptote in kcal/mol. The energies obtained from the PES are given in blue, and their ZPE-corrected values are shown in red italic.

below, these observations are indeed born out from our dynamics calculations on a recently developed global potential energy surface (PES). We, further, demonstrate that it is possible to control the relative contributions of the two pathways by exciting a vibrational mode of the HO_2 reactant, which also leads to drastically different product state distributions.

In 1998, Varandas and co-workers[18] published a pioneering study on the dynamics of $O + HO_2$ reaction, reporting the ro-vibrational distributions OH and O_2 at the collision energy of $E_c = 4.184$ kJ/mol. Using a quasi-classical trajectory (QCT) method, the dynamical calculations were performed on the first full-dimensional PES for this system, which was fitted using the double many-body expansion (DMBE) method to *ab initio* points calculated using unrestricted configuration interaction with single and double excitations (UCISD) and the 6-311G++(d, p) basis set.[18] On this DMBE I PES, the majority of the OH product were found in the vibrational ground state, via the OA pathway. In 2004, these authors further studied the role of HO_2 vibrational excitation in the title reaction on the DMBE I PES[17] and an improved DMBE II PES[19] and concluded that the impact of HO_2 vibrational excitation is relatively minor even for highly vibrationally excited HO_2.[20] The DMBE PESs have also been used in transition-state theory calculations of the rate coefficients, but the results are not in good agreement with known experimental values.[21]

Very recently, we have developed a more accurate full-dimensional global PES for the HO_3 system constructed from more than 21 000 multireference configuration interaction (MRCI) points,[22,23] using the high-fidelity permutation invariant polynomial-neural network (PIP-NN) method.[24] The active space used in the CASSCF calculations includes 13 electrons in 10 orbitals with 1s and 2s orbitals of O atoms closed, while the full-valence active space was used in subsequent MRCI calculations. The MRCI treatment of the PES was found to be essential due to the strongly correlated nature of this system.[25,26] This new PES has been demonstrated to reproduce various spectroscopic, kinetic, and dynamics properties of the system.[22,23,27,28] In several comparisons, the results on the new PES were found to differ significantly from those obtained from the DMBE PESs,[17,19] presumably due to the neglect of multireference effects in the

earlier *ab initio* calculations and the relatively small number of *ab initio* points used in the DMBE fitting. As a result, it is not clear if the previous dynamics results for the title reaction obtained from the DMBE PESs are reliable. In this Letter, we report a detailed QCT dynamical study of R1 on our new PES, focusing on the impact of vibrational excitation of the HO_2 reactant on the reaction mechanism as well as the product internal distributions, which might impact atmospheric modeling.

Standard QCT calculations were performed using VENUS[29] on the PIP-NN PES with the reactants prepared in various vibrational states. For each vibrational state of HO_2, the normal mode coordinates and momenta were transformed to the atomic counterparts.[30] The initial relative translational energy and initial rotational energies of reactants were sampled from the Boltzmann distribution at 200 K, which is relevant for the atmospheric conditions. 120 000 trajectories were propagated for each vibrational state with a time step of 0.1 fs and the maximum impact parameter b_{max} of 5.5 Å. The vibrational state distributions of the diatomic products were obtained using the Einstein–Brillouin–Keller method,[31] by binning the vibrational actions to the nearest integers. Mechanistic insights on the particular pathway taken by a trajectory can be readily identified by examining the connectivity of the products ($HO_a + O_bO_c$ and $HO_b + O_aO_c$ for the HA and OA channels, respectively.) In reality, such channels can be distinguished by isotope labeling, as done by Sridharan et al.[32]

The energetics of the title reaction on the PIP-NN PES is shown in Figure 1, including all calculated geometries and energies of stationary points along both the HA and OA pathways. The detailed structures and harmonic frequencies of stationary points are listed in Tables S1 and S2, respectively. The agreement with available experimental data[33,34] is quite good, which is a testament of the quality of the PES. The title reaction is highly exoergic, with a reaction energy of −52.91 kcal/mol with zero-point energy (ZPE) corrections, which allows the highest accessible vibrational level of $v = 6$ or $v = 13$ for the OH or O_2 product. For the reactant HO_2, the OH stretching mode (v_1) has the highest calculated harmonic frequency of 3658.7 cm^{-1}, while the bending mode (v_2) and

OO stretching mode (v_3) are 1431.9 and 1116.7 cm^{-1}, respectively, in reasonably good agreement with experiment.

At 200 K, which is relevant to atmospheric chemistry, the HA pathway is essentially closed for the HO$_2$ radical in the vibrational ground state, consistent with the isotopic experiment of Sridharan et al.,[32] who found no participation of the HA channel at room temperature. At room temperature, the calculated rate coefficient is 2.17×10^{-11} cm^3 s^{-1}, which compares reasonably well with the experimental values of $5-6 \times 10^{-11}$ cm^3 s^{-1},[32] further validating the accuracy of the PES.

The calculated rate coefficients of the two pathways at 200 K for HO$_2$ in both the ground and excited vibrational states are shown in Table 1. The reaction is completely dominated by

Table 1. Rate Coefficients (cm^3 s^{-1}) under Different Vibrational Excitations at 200 K

HO$_2$ mode	quantum number	H abstraction	O abstraction	total
	$v = 0$	2.13×10^{-14}	2.22×10^{-11}	2.22×10^{-11}
OH stretch	$v_1 = 1$	7.80×10^{-12}	2.17×10^{-11}	2.95×10^{-11}
	$v_1 = 2$	2.95×10^{-11}	1.63×10^{-11}	4.58×10^{-11}
	$v_1 = 3$	3.37×10^{-11}	1.56×10^{-11}	4.93×10^{-11}
bend	$v_2 = 1$	5.84×10^{-14}	2.22×10^{-11}	2.23×10^{-11}
OO stretch	$v_3 = 1$	6.74×10^{-14}	2.29×10^{-11}	2.30×10^{-11}

the OA channel when HO$_2$ is in its vibrational ground state, as HA channel constitutes only a tiny percentage. It is also clear from the table that the excitation of either the bending (v_2) or OO stretching (v_3) mode of HO$_2$ has little effect on the rate coefficients as the HA channel remains closed. However, the HA rate coefficient increases drastically with the excitation of the OH stretching mode (v_1) of the HO$_2$ reactant, while the OA reaction rate decreases at the same time. When the OH mode is excited beyond its first overtone, the HA channel becomes the dominant one, accompanied by an increased total rate. Our observations are in sharp contrast to the earlier work of Varandas and co-workers, who reported almost no vibrational enhancement of the reactivity.[20]

The effectiveness of the v_1 mode of the HO$_2$ reactant in promoting the HA channel can be readily understood in terms of the Sudden Vector Projection (SVP) model,[35] which stipulates that mode specificity of a chemical reaction is controlled by the projection of the corresponding reactant normal mode vector onto the reaction coordinate at the relevant transition state. The SVP model has been successfully applied to many direct reactions in which the sudden conditions are satisfied.[36] In Table 2, the SVP values for various reactant modes are listed for the HA channel and it can be readily seen that the reaction coordinate at SP2 is well aligned with the v_1 mode of HO$_2$, reflected by a large SVP value of 0.745. The impact of exciting the v_2 or v_3 mode is moderate, consistent with the slightly increased rate coefficient for this channel. On the other hand, none of the HO$_2$ vibrational modes is very effective in promoting the OA channel.

The calculated vibrational distributions for the OH and O$_2$ products from different initial states at 200 K are shown in the Figures 2 and 3, respectively. For comparison, the theoretical results of Varandas and co-workers on the DMBE I PES[18] and the DMBE II PES[20] are also included in figures, which were calculated for the ground HO$_2$ vibrational state (panel a) and for $E_{vib} = 48.0$ kcal/mol (panel d).

Table 2. SVP Projections for the Reactant and Product Modes of the O + HO$_2 \rightarrow$ OH + O$_2$ Reaction for the HA and OA Channels

species	mode	H abstraction	O abstraction
reactant	relative translation	0.453	0.229
HO$_2$	OH stretch (v_1)	0.745	0.004
HO$_2$	bend (v_2)	0.464	0.012
HO$_2$	OO stretch (v_3)	0.321	0.001
product	relative translation	0.258	0.301
OH	rotation	0.147	0.022
OH	vibration	0.950	0.006
O$_2$	rotation	0.026	0.236
O$_2$	vibration	0.130	0.540

For the reaction from the vibrational ground state of HO$_2$, it is clear that the OH product is almost exclusively in its vibrational ground state, while the vibration of the O$_2$ product is highly excited. Our results are similar to the 1998 values of Varandas and co-workers[18] but quite different from their 2004 results.[20] The inconsistent OH distributions in the previous theoretical calculations are probably attributable to large differences in the two DMBE PESs used in the calculations. Our product vibrational distributions can also be explained by the SVP model, which takes advantage of the microscopic reversibility in predicting the product energy disposal.[36] As shown in Table 2, the O$_2$ vibrational mode has a good overlap with the reaction coordinate at SP1 for the OA channel, which dominates the reaction under thermal conditions. For this saddle point, on the other hand, the OH vibration has a small SVP value as it is essentially a spectator in the OA channel.

For reaction with the v_1 mode of HO$_2$ excited, the OH product distribution becomes bimodal, as shown in Figure 3. The peak for the low-lying states is clearly correlated with the OA channel, where the OH moiety is a spectator and its excitation is largely preserved, as discussed above. On the other hand, populations at high vibrational states of the OH product are associated with the HA pathway, which can also be rationalized by the SVP model. As shown in Table 2, the SVP value for the vibrational mode of the OH product is quite large at SP2, as the H abstraction requires the motion of the transfer H atom. In addition, the amount of vibrational excitation in the OH product is also proportional to the increasing v_1 quantum number. Interestingly, we note that the OH vibrational distribution reported by Varandas and co-workers[20] for a vibrational energy of 48.0 kcal/mol evenly distributed in the three vibrational modes of HO$_2$ is a monotonically decay function of the OH vibrational quantum, in sharp contrast to our results. For the O$_2$ product, on the other hand, the dominance of the HA channel for reaction with v_1 excited HO$_2$ also leads to a bimodal structure in the O$_2$ vibrational distribution. A monotonically decay component at low vibrational states is obviously due to the emergence of the HA channel. This can be rationalized by the small SVP value of the O$_2$ vibrational mode in this channel. The highly vibrationally excited O$_2$ from the OA channel are found to have a diminishingly small contribution to the overall vibrational distribution due to a decreasing importance of this channel with increasing v_1 excitation in the HO$_2$ reactant.

The poor agreement between the vibrational distributions calculated on our new PES and those reported previous by Varandas and co-workers,[18,20] is likely due to inaccuracies in the two DMBE PESs. On our PES, the submerged saddle point
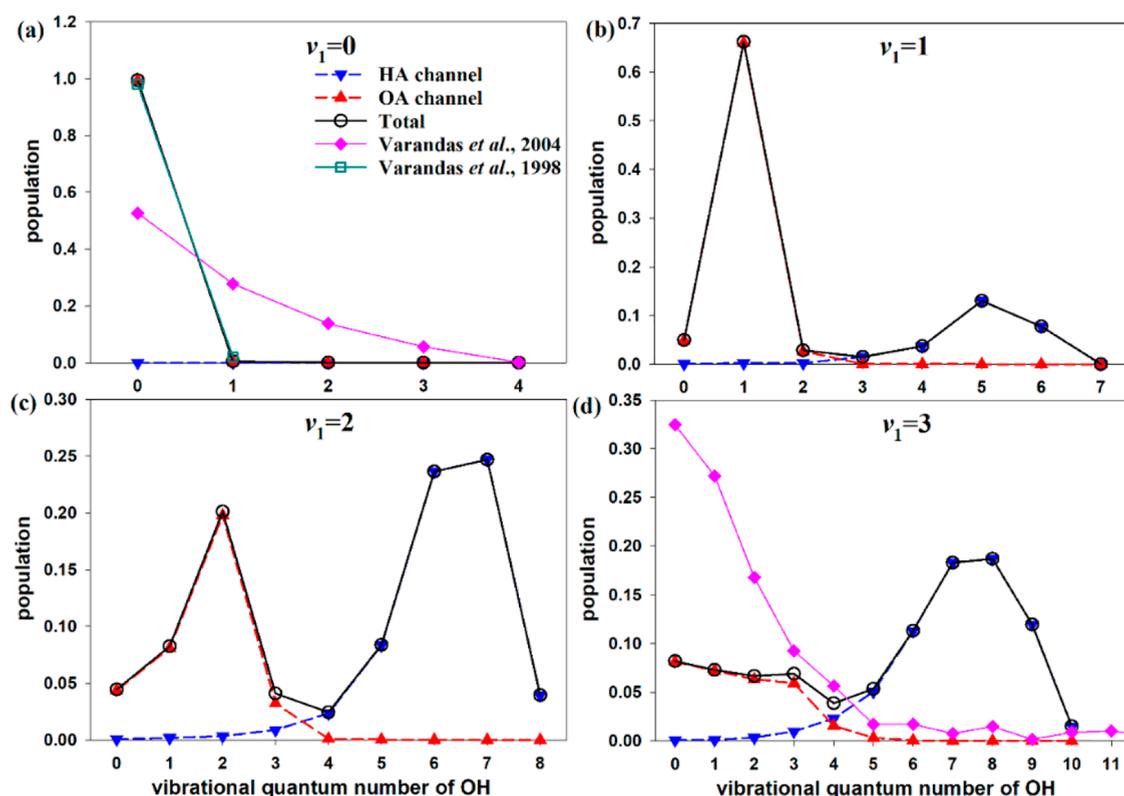
Figure 2. Calculated vibrational distributions of the product OH from different initial vibrational excitations in the OH stretching mode (v_1) of the reactant HO_2. The previous theoretical distributions of Varandas and co-workers[18,20] are also shown for comparison.
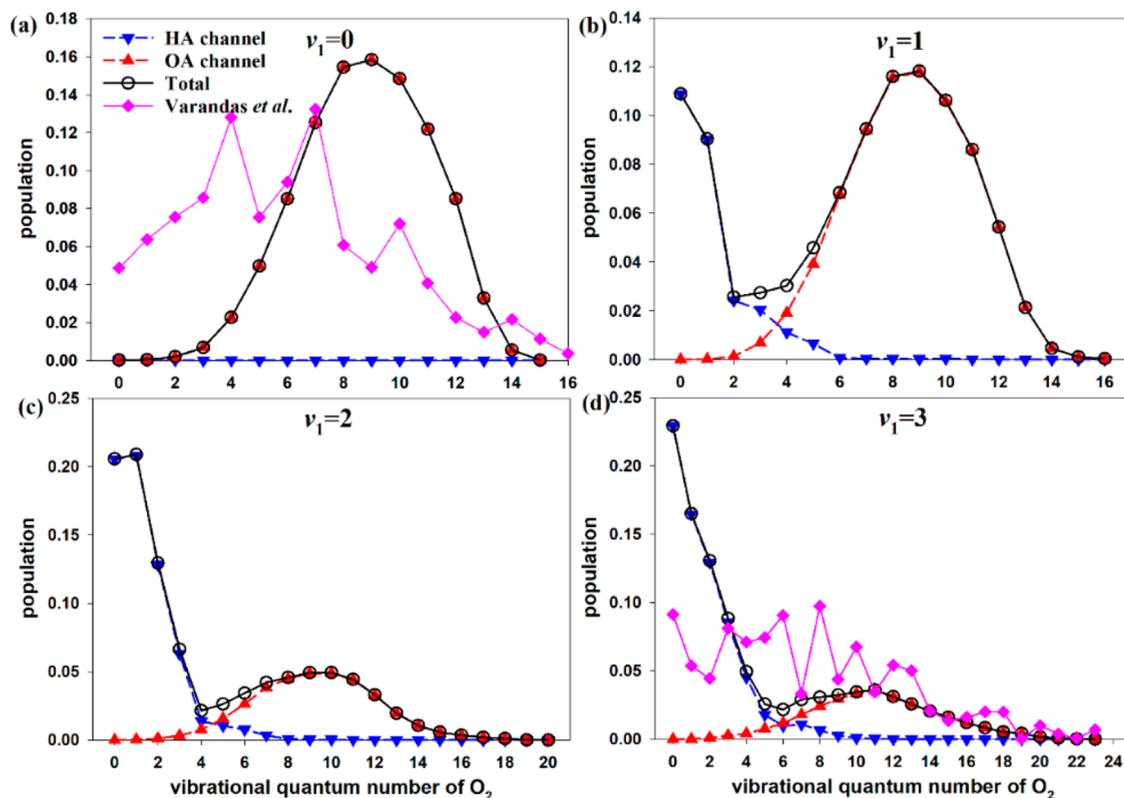
Figure 3. Calculated vibrational distributions of the product O_2 from different initial vibrational excitations in the OH stretching mode (v_1) of the reactant HO_2. The previous theoretical distributions of Varandas and co-workers[20] are also shown for comparison.

in the OA channel is 1.78 kcal/mol lower than the reactant asymptote, accessible from a vdW well, which is 3.08 kcal/mol

below the reactant asymptote. For the DMBE I PES, however, the vdW well is only 1.39 kcal/mol below the reactants, which
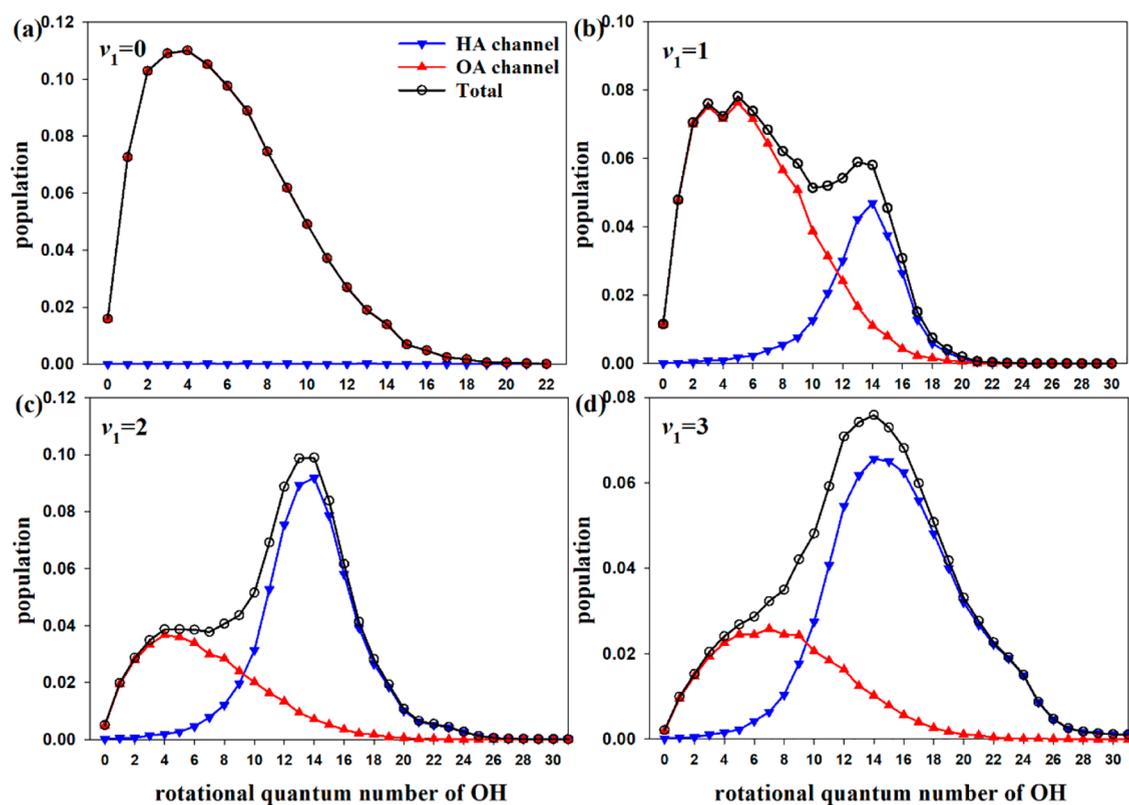
Figure 4. Calculated rotational distributions of the product OH from different initial vibrational excitations in the OH stretching mode (v_1) of the reactant HO_2.
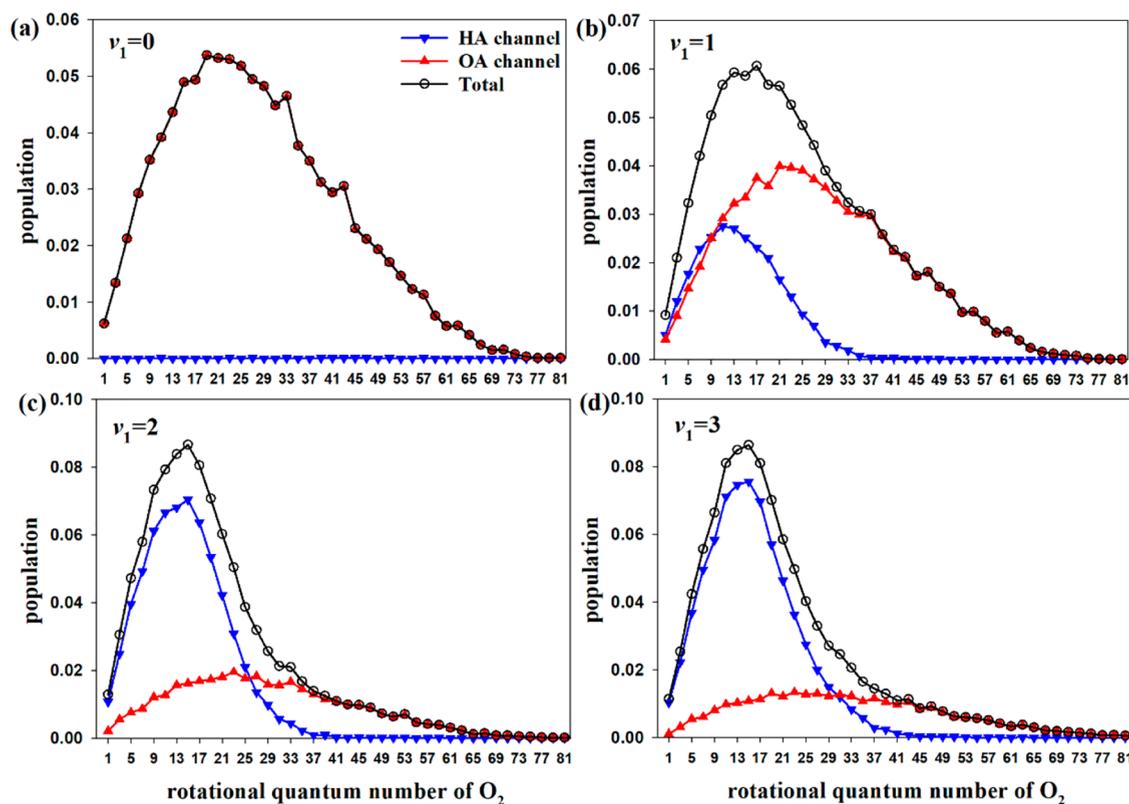
Figure 5. Calculated rotational distributions of the product O_2 from different initial vibrational excitations in the OH stretching mode (v_1) of the reactant HO_2. Only odd quantum numbers are included assuming the oxygen is the ^{16}O isotope in the ground electronic state, for which the even quantum numbers are not allowed because of its bosonic nuclear spin.

impacts the dynamics at low collision energies.[17,21] When it comes to the HA channel, the barrier height of SP2 was controversial for many years.[16−21,25] Our new PIP-NN PES shows a very tight saddle point, which has a barrier of 6.96 kcal/mol,[23] significantly lower than the 17.9 kcal/mol value reported by Varandas and co-workers.[17] We have, further, examined the barrier height by recalculating the minimum energy path using a larger basis set. The barrier obtained at the level of MRCI-F12/VQZ-F12 is only 0.96 kcal/mol higher than the value of our PES, as discussed in the Supporting Information. These are only some representations of the differences between the PESs.

Figures 4 and 5 examine the rotational energy disposal in the products. It is clear that the rotational excitation in the OH and O_2 products is also closely related to the two reaction pathways. For the OA channel, the rotational excitations in both OH and O_2 are moderate. For the HA channel, on the other hand, OH radicals are significantly more excited in their rotational degrees of freedom. The relative contributions of the two channels to the rotational distributions are clearly observable in the figures. As shown in the Table 2, the SVP model also predicts how much the energy flows into the rotational modes. For the OA channel, the O_2 rotation is more easily excited than the OH rotation, meanwhile, a reversal occurs for the HA channel. In SI, the energy partition in the products along the different reaction pathways is listed in Table S3.

The results reported here have important implications in the origin of the OH based nightglow. From our results, it is clear that the title reaction at 200 K will hardly produce any OH with $v > 1$. However, highly excited OH up to $v = 9$ can be produced if the HO_2 reactant has excitation in its v_1 mode. Such vibrationally hot HO_2 may indeed exist in the atmosphere, via for example the OH + O_3 → HO_2 + O_2 reaction, as pointed out by Varandas and co-workers.[37−39] Although little direct evidence exists for a significant presence of v_1-excited HO_2 in the middle atmosphere, it is possible such scenarios are relevant in local thermodynamic disequilibrium situations.[40] In such cases, the contribution of the HA channel should be included in the atmospheric model. For situations at thermal equilibrium, the nightglow is most likely due to the H + O_3 → OH(v) + O_2 reaction, which occurs on the same PES.[27]

In summary, we investigated the detailed dynamics of the O + HO_2 → OH + O_2 reaction using a QCT method on a recently developed PIP-NN PES to obtain nascent ro-vibrational distributions of the two products and to understand their dynamical origins. To explore vibrational control of two reaction pathways to the same products, we show that the excitation of the v_1 vibrational mode of HO_2 opens the HA channel, which has a higher barrier, and significantly enhances the reaction rate. The v_1 excitation of the reactant also leads to highly vibrationally exited OH product, as the reaction coordinate at the corresponding transition state is strongly aligned with the OH vibration, leading to facile energy disposal into this mode. This study thus presents an example how the vibrational excitation in the reactant controls product formation.

The elucidation of the dynamics of the O + HO_2 reaction helps to shed valuable light on its role in Earth's stratosphere and mesosphere. Under atmospheric conditions, our results indicate that the OH product is mostly in its vibrational ground state with moderate rotational excitation, thanks to the spectator nature of the OH in the barrierless OA channel, which dominates the reaction at low temperatures. Hence, our results do not support the hypothesis that the title reaction produces vibrationally excited OH radicals that are responsible for OH nightglow, unless vibrationally hot HO_2 are involved.

■ ASSOCIATED CONTENT

ⓈI Supporting Information

The Supporting Information is available free of charge at https://pubs.acs.org/doi/10.1021/acs.jpclett.2c00053.

> Additional information for the potential energy surface and energy partition in the products (PDF)

■ AUTHOR INFORMATION

Corresponding Author

Xixi Hu − *Kuang Yaming Honors School, Institute for Brain Sciences, Nanjing University, Nanjing 210023, China;* ⓞ orcid.org/0000-0003-1530-3015; Email: xxhu@ nju.edu.cn

Authors

Qixin Chen − *Institute of Theoretical and Computational Chemistry, Key Laboratory of Mesoscopic Chemistry, School of Chemistry and Chemical Engineering, Nanjing University, Nanjing 210023, China;* ⓞ orcid.org/0000-0002-1768-8732

Shuwen Zhang − *Institute of Theoretical and Computational Chemistry, Key Laboratory of Mesoscopic Chemistry, School of Chemistry and Chemical Engineering, Nanjing University, Nanjing 210023, China*

Daiqian Xie − *Institute of Theoretical and Computational Chemistry, Key Laboratory of Mesoscopic Chemistry, School of Chemistry and Chemical Engineering, Nanjing University, Nanjing 210023, China;* ⓞ orcid.org/0000-0001-7185-7085

Hua Guo − *Department of Chemistry and Chemical Biology, University of New Mexico, Albuquerque, New Mexico 87131, United States;* ⓞ orcid.org/0000-0001-9901-053X

Complete contact information is available at:
https://pubs.acs.org/10.1021/acs.jpclett.2c00053

Notes

The authors declare no competing financial interest.

■ REFERENCES

(1) Levine, R. D. *Molecular Reaction Dynamics*; Cambridge University Press: Cambridge, 2005.

(2) Casavecchia, P.; Leonori, F.; Balucani, N. Reaction dynamics of oxygen atoms with unsaturated hydrocarbons from crossed molecular beam studies: primary products, branching ratios and role of intersystem crossing. *Int. Rev. Phys. Chem.* **2015**, *34*, 161−204.

(3) Guo, H.; Liu, K. Control of chemical reactivity by transition state and beyond. *Chem. Sci.* **2016**, *7*, 3992−4003.

(4) Pan, H.; Liu, K.; Caracciolo, A.; Casavecchia, P. Crossed beam polyatomic reaction dynamics: recent advances and new insights. *Chem. Soc. Rev.* **2017**, *46*, 7517−7547.

(5) Li, J.; Zhao, B.; Xie, D.; Guo, H. Advances and new challenges to bimolecular reaction dynamics theory. *J. Phys. Chem. Lett.* **2020**, *11*, 8844−8860.

(6) Lu, D.; Li, J.; Guo, H. Stereodynamical control of product branching in multi-channel barrierless hydrogen abstraction of CH_3OH by F. *Chem. Sci.* **2019**, *10*, 7994−8001.

(7) Bates, D. R.; Nicolet, M. The photochemistry of atmospheric water vapor. *J. Geophys. Res.* **1950**, *55*, 301−327.

(8) Takahashi, H.; Batista, P. P. Simultaneous measurements of OH(9,4), (8,3), (7,2), (6,2) and (5,1) bands in the airglow. *J. Geophys. Res. Space Phys.* **1981**, *86*, 5632−5642.

(9) Turnbull, D. N.; Lowe, R. P. Vibrational population distribution in the hydroxyl night airglow. *Can. J. Phys.* **1983**, *61*, 244−250.

(10) Lopez-Moreno, J. J.; Rodrigo, R.; Moreno, F.; Lopez-Puetas, M.; Molina, A. Altitude distribution of vibrationally excited states of atmospheric hydroxyl at levels v = 2 to v = 7. *Planet. Space Sci.* **1987**, *35*, 1029−1038.

(11) Sivjee, G. G.; Hamwey, R. M. Temperature and chemistry of the polar mesopause OH. *J. Geophys. Res. Space Phys.* **1987**, *92*, 4663−4672.

(12) Llewellyn, E. J.; Long, B. H.; Solheim, B. H. The quenching of OH* in the atmosphere. *Planet. Space Sci.* **1978**, *26*, 525−531.

(13) McDade, I. C.; Llewellyn, E. J. Kinetic parameters related to sources and sinks of vibrationally excited OH in the nightglow. *J. Geophys. Res. Space Phys.* **1987**, *92*, 7643−7650.

(14) Kaye, J. A. On the possible role of the reaction O + HO_2 → OH + O_2 in OH airglow. *J. Geophys. Res.* **1988**, *93*, 285−288.

(15) Xu, J.; Gao, H.; Smith, A. K.; Zhu, Y. Using TIMED/SABER nightglow observations to investigate hydroxyl emission mechanisms in the mesopause region. *J. Geophys. Res. Atmos.* **2012**, *117*, D02301.

(16) Dupuis, M.; Fitzgerald, G.; Hammond, B.; Lester, W. A.; Schaefer, H. F. Theoretical study of the H+O_3↔OH+O_2↔O+HO_2 system. *J. Chem. Phys.* **1986**, *84*, 2691−2697.

(17) Varandas, A. J. C.; Yu, H. G. Double many-body expansion potential energy surface for ground-state HO_3. *Mol. Phys.* **1997**, *91*, 301−318.

(18) Wang, W.; González-Jonte, R.; Varandas, A. J. C. Quasiclassical trajectory study of the environmental reaction O + HO_2 → OH + O_2. *J. Phys. Chem. A* **1998**, *102*, 6935−6941.

(19) Yu, H.-G.; Varandas, A. J. C. Ab initio theoretical calculation and potential energy surface for ground-state HO_3. *Chem. Phys. Lett.* **2001**, *334*, 173−178.

(20) Silveira, D. M.; Caridade, P. J. S. B.; Varandas, A. J. C. Dynamics study of the O + HO_2 reaction using two DMBE potential energy surfaces: The role of vibrational excitation. *J. Phys. Chem. A* **2004**, *108*, 8721−8730.

(21) Fernández-Ramos, A.; Varandas, A. J. C. A VTST study of the H + O_3 and O + HO_2 reactions using a six-dimensional DMBE potential energy surface for ground state HO_3. *J. Phys. Chem. A* **2002**, *106*, 4077−4083.

(22) Hu, X.; Zuo, J.; Xie, C.; Dawes, R.; Guo, H.; Xie, D. An ab initio based full-dimensional potential energy surface for OH + O_2 ⇄ HO_3 and low-lying vibrational levels of HO_3. *Phys. Chem. Chem. Phys.* **2019**, *21*, 13766−13775.

(23) Zuo, J.; Chen, Q.; Hu, X.; Guo, H.; Xie, D. Theoretical investigations of rate coefficients for H + O_3 and HO_2 + O reactions on a full-dimensional potential energy surface. *J. Phys. Chem. A* **2020**, *124*, 6427−6437.

(24) Jiang, B.; Li, J.; Guo, H. Potential energy surfaces from high fidelity fitting of ab initio points: The permutation invariant polynomial-neural network approach. *Int. Rev. Phys. Chem.* **2016**, *35*, 479−506.

(25) Setokuchi, O.; Sato, M.; Matuzawa, S. A theoretical study of the potential energy surface and rate constant for an $O(^3P)$ + HO_2 reaction. *J. Phys. Chem. A* **2000**, *104*, 3204−3210.

(26) Varandas, A. J. C. Odd-hydrogen: An account on electronic structure, kinetics, and role of water in mediating reactions with atmospheric ozone. Just a catalyst or far beyond? *Int. J. Quantum Chem.* **2014**, *114*, 1327−1349.

(27) Chen, Q.; Hu, X.; Guo, H.; Xie, D. Insights into the formation of hydroxyl radicals with nonthermal vibrational excitation in the Meinel airglow. *J. Phys. Chem. Lett.* **2021**, *12*, 1822−1828.

(28) Chen, Q.; Hu, X.; Guo, H.; Xie, D. Theoretical H + O_3 rate coefficients from ring polymer molecular dynamics on an accurate global potential energy surface: assessing experimental uncertainties. *Phys. Chem. Chem. Phys.* **2021**, *23*, 3300−3310.

(29) Hu, X.; Hase, W. L.; Pirraglia, T. Vectorization of the general Monte Carlo classical trajectory program VENUS. *J. Comput. Chem.* **1991**, *12*, 1014−1024.

(30) Hase, W. L. Classical trajectory simulations: Initial conditions. In *Encyclopedia of Computational Chemistry*; Alinger, N. L., Ed.; Wiley, 1998; Vol. *1*, pp 399−402.

(31) Gutzwiller, M. C. *Chaos in Classical and Quantum Mechanics*; Springer: New York, 1990.

(32) Sridharan, U. C.; Klein, F. S.; Kaufman, F. Detailed course of the O+HO_2 reaction. *J. Chem. Phys.* **1985**, *82*, 592−593.

(33) Huber, K. P.; Herzberg, G. *Molecular Spectra and Molecular Structure, IV, Constants of Diatomic Molecules*; Van Norstrand Reinhold: New York, 1979.

(34) Jacox, M. E. Vibrational and electronic energy levels of polyatomic transient molecules: Supplement 1. *J. Phys. Chem. Ref. Data* **1990**, *19*, 1387−1546.

(35) Jiang, B.; Guo, H. Relative efficacy of vibrational vs. translational excitation in promoting atom-diatom reactivity: Rigorous examination of Polanyi's rules and proposition of sudden vector projection (SVP) model. *J. Chem. Phys.* **2013**, *138*, 234104.

(36) Guo, H.; Jiang, B. The sudden vector projection model for reactivity: Mode specificity and bond selectivity made simple. *Acc. Chem. Res.* **2014**, *47*, 3679−3685.

(37) Zhang, L.; Varandas, A. J. C. Dynamics of the OH(v = 1,2,4) + O_3 atmospheric reaction. *Phys. Chem. Chem. Phys.* **2001**, *3*, 1439−1445.

(38) Varandas, A. J. C. On the "ozone deficit problem": What are O_x and HO_x catalytic cycles for ozone depletion hiding? *ChemPhysChem* **2002**, *3*, 433−441.

(39) Varandas, A. J. C. Are vibrationally excited molecules a clue for the "O_3 deficit problem" and "HOx dilemma" in the middle atmosphere? *J. Phys. Chem. A* **2004**, *108*, 758−769.

(40) Varandas, A. J. C. Steady-state distributions of O_2 and OH in the high atmosphere and implications in the ozone chemistry. *J. Phys. Chem. A* **2003**, *107*, 3769−3777.